Available online at www.sciencedirect.com
ScienceDirect
Cement and Concrete Research 37 (2007) 957–971
Cement and Concrete Research

A method for mix-design of fiber-reinforced self-compacting concrete

Liberato Ferrara [a,b,*], Yon-Dong Park [b,c], Surendra P. Shah [d]

[a] Department of Structural Engineering, Politecnico di Milano, piazza Leonardo da Vinci, 20133 Milano, Italy
[b] Center for Advanced Cement Based Materials (ACBM), Northwestern University, USA
[c] Faculty of Construction and Architectural Design, Daegu Haany University, South Korea
[d] Walter P. Murphy Professor of Civil Engineering, Director of Center for ACBM, Northwestern University, 2145 Sheridan Road, Suite A130, 60201 Evanston, IL, USA

Received 19 September 2006; accepted 28 March 2007

Abstract

The addition of fibers to self-compacting concrete (SCC) may take advantage of its superior performance in the fresh state to achieve a more uniform dispersion of fibers, which is critical for a wider structural use of fiber-reinforced concrete. Some useful, mainly empirical, guidelines are available for mix design of fiber-reinforced SCC. In this work a "rheology of paste model" is applied to the mix design of Steel Fiber Reinforced SCC (SFRSCC). Fibers are included in the particle size distribution of the solid skeleton through the concept of an equivalent diameter, defined on the basis of the specific surface. The influence of fibers (type and quantity) on the grading of solid skeleton, minimum content and rheological properties of the paste required to achieve the required self-compactability and rheological stability were studied. Tests were conducted on both plain and fiber-reinforced concrete made with a variety of mix compositions. In addition, rheological tests were made with corresponding cement pastes.

Keywords: Rheology; Mixture proportioning; Fresh concrete; Cement paste; Self-compacting concrete; Fiber reinforcement

1. Introduction

Self-compacting concrete (SCC) is featured in its fresh state by high flowability and rheological stability. SCC has excellent applicability for elements with complicated shapes and congested reinforcement. The addition of fibers into self-compacting concrete may take advantage of its high performance in the fresh state to achieve a more uniform dispersion of fibers, which is critical for a wider and reliable structural use of fiber-reinforced cement composites. The compactness of the SCC matrix, due to the higher amount of fine and extra-fine particles, may improve interface zone properties [1], and consequently also the fiber-matrix bond, leading to enhanced post-cracking toughness and energy absorption capacity. The synergy between self-compacting and fiber-reinforced technologies, thanks to the elimination of vibration and the reduction or even the complete substitution of conventional reinforcement with fibers, is likely to improve the economic efficiency of the construction process. Increased speed of construction, reduction or suitably focused rearrangement of labor resources, costs and energy consumption, better working environment, with reduced noise and health hazards, also contribute toward the automation and reliability of quality control.

A considerable amount of research work has been devoted over the last decade to make self-compacting concrete more robust [2]. Design methods found in the literature often seek separate optimization of the paste composition and granular skeleton grading. The former is usually based on fluidity requirements, in which the cement content and the water/binder ratio have also to comply with minimum strength and durability requirements [3,4]. For the grading of granular skeleton, recommendations on the maximum aggregate diameter and on the fine to coarse aggregate ratio have been provided to achieve the optimum packing density [3–5]. De Larrard applied to the

* Corresponding author. Department of Structural Engineering, Politecnico di Milano, piazza Leonardo da Vinci, 20133 Milano, Italy. Tel.: +39 02 23994387; fax: +39 02 23994220.
E-mail addresses: liberato.ferrara@polimi.it (L. Ferrara), s-shah@northwestern.edu (S.P. Shah).

0008-8846/$ - see front matter © 2007 Elsevier Ltd. All rights reserved.
doi:10.1016/j.cemconres.2007.03.014

design of SCC his compressible packing model [6,7]. Saak et al. [8] proposed a model in which the yield stress and viscosity of the cement paste are optimized with respect to static and dynamic segregation of coarser aggregate particles. Bui et al. [9] further extended the model by relating the rheological properties of cement paste to the size distribution and void ratio of the solid particles and to the paste volume ratio. Factorial design models have been also applied to mix design of SCC [10,11], deriving design charts which correlate input mix-design variables to output material properties, mainly consisting of the measurements of fresh state properties as well as the compressive strength. Useful correlation between different measurements of fresh state behavior has also been provided [12–15], in an attempt to make them more closely representative of fundamental rheological properties of fluid concrete [16–19].

As for the inclusion of the fibers into the mix design, De Larrard [6] proposed the concept of a perturbation volume for his compressible packing model. Yu et al. [20,21] defined an "equivalent packing diameter" which relates the dimensions of a non-spherical particle to a fictitious sphere having a diameter that does not result in a change in the packing density. Grünewald [22] defined the "maximum fiber factor", related to the content and particle size distribution of the aggregates and their risk of blocking through an equivalent bar spacing which is actually the ratio of the fiber length to the maximum aggregate diameter. Bui et al. [23] also attempted to include the contribution of fibers into the rheological paste model through the optimization of the packing density of the fiber-reinforced solid skeleton and the definition of an average excess thickness of the paste/mortar, defined as the ratio between the paste/mortar volume and the total surface area of coarse aggregates and fibers. A correlation between rheological properties of mortar (max aggregate size 2 mm) and its excess thickness proved satisfactory. However, application to concrete is still lacking.

In this work the rheological paste model [8,9] is applied to the design of steel fiber-reinforced self-compacting concrete (SFR-SCC). The key idea is to include the fibers in the particle size distribution of the solid skeleton through the concept of an equivalent diameter, defined on the basis of the specific surface area of the fiber reinforcement. Through rheology tests on cement pastes and tests on both plain and fiber-reinforced concrete, the influence of fibers on the interparticle void, average diameter and spacing of the solid particles, and hence on the requirements on the minimum paste content and rheological properties of the paste to achieve the required fresh state performance were evaluated. The rheological properties of the concrete may also influence the dispersion and orientation of fibers and, as a consequence, the toughness characteristics of the hardened composite [22,24–28]. This has been regarded as outside the main scope of this work and will form the subject of a further investigation.

2. Review of the rheological paste model for SCC proportioning

The "rheology of the paste model" for proportioning SCC was originally developed by Saak et al. [8]. They derived theoretical equations for a single spherical particle suspended in the fluid cementitious paste under the assumption that a minimum yield stress and viscosity of the cement paste, also as a function of the density difference between the particle and the paste itself, are required in order to avoid segregation under both static and dynamic conditions. An experimentally calibrated upper bound for both yield stress and viscosity of cement paste to avoid poor deformability of concrete allowed the definition of a self-flow zone. Bui et al. [9] expanded these concepts to include the effects of aggregate (and paste) volume ratio, particle size distribution of the aggregates and fine to coarse aggregate ratio. These factors, together with the aggregate shape, influence the void content and the average diameter of the solid skeleton particles, the last being defined as:

$$d_{av} = \frac{\sum_i d_i m_i}{\sum_i m_i} \quad (1)$$

where d_i is the average diameter of aggregate fraction i (defined as the average opening size of two consecutive sieves) and m_i is the mass of that fraction, i.e. the mass retained at the lower opening sieve.

A minimum volume of cementitious paste is needed to fill the voids between the aggregate particles and create a layer enveloping the particles, thick enough to ensure the required deformability and segregation resistance of concrete. A further parameter is hence defined as key to the model, i.e. the average aggregate spacing d_{ss}, defined as twice the thickness of the excess paste layer enveloping the aggregates:

$$d_{ss} = d_{av}\left[\sqrt[3]{1+\frac{V_{paste}-V_{void}}{V_{concrete}-V_{paste}}}-1\right] \quad (2)$$

This can be hence regarded as an indicator of the "degree of suspension" of the given solid skeleton, featured by its own particle size distribution — average aggregate size d_{av} — and void ratio in the densely compacted state, into a certain volume of cement paste. The rheological properties of the paste (yield stress and viscosity) have to be optimized with respect to the average aggregate diameter and as a function of the aggregate spacing. As shown in Fig. 1 and as it will be further explained in details, for a given aggregate grading, i.e. for a certain value of the average aggregate diameter, a higher average aggregate spacing (which would mean lower aggregate content and hence higher paste content) requires a lower flow diameter (higher yield stress) and a higher viscosity of the paste to obtain the desired fluidity and rheological stability (resistance to segregation) characteristics.

2.1. Extension of the rheological paste model to fiber-reinforced concretes

In this framework the design of fiber-reinforced self-compacting concrete is performed by first providing a separate optimization of the particle size distribution of the solid skeleton

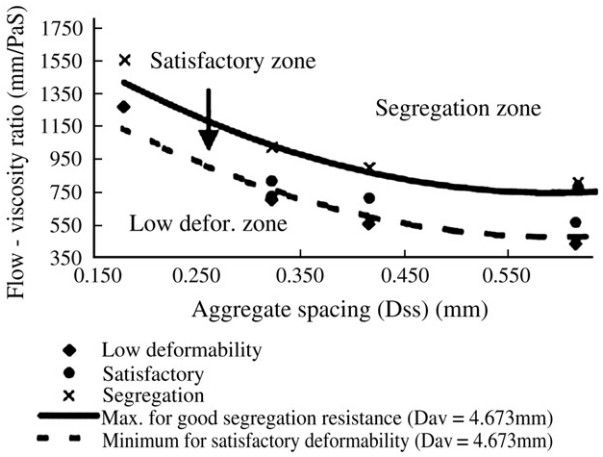

Fig. 1. Model lines for flow viscosity ratio of experimental data and aggregate spacing d_{ss} (average diameter d_{av}=4.673 mm) — from [9].

and of the paste rheology, further assessing the correlation between them to the achievement of the desired fresh state behavior of the material. With reference to the former task, once the fine and coarse aggregate are chosen and the particle size distribution for each one determined, e.g. according to ASTM C136 or EN 933-1 [29,30], the optimization of the solid skeleton can be performed through one of the grading curves commonly employed in the design of ordinary concrete mixes. In this work the curve proposed by Funk and Dinger [31] has been employed:

$$P(d) = \frac{d^q - d_{\min}^q}{d_{\max} - d_{\min}^q} \tag{3}$$

where $P(d)$ gives the cumulative passing fraction at a sieve with opening d, $d_{\max}$ is the maximum aggregate diameter and $d_{\min}$ has been chosen, at this stage, equal to the minimum sieve diameter employed for the particle size analysis of the aggregates (usually $d_{\min}$=0.075 mm). For $d_{\min}$=0 and q=0.5 Eq. (1) gives back the well known Fuller and Thompson's curve, which is known to perform poorly in the extra-fine particle region because of the lack of a proper characterization of coarse and fine aggregates in that region. As for the value of factor q, it has been claimed that the use of q=0.37 yields the best packing density [32]. Actually, lower q values give better curve performance in accounting for fine and extra-fine fractions, provided their proper particle size distribution has been obtained. Brouwers and Radix [4] in fact showed that q=0.25 is the most suitable value to get the actual distribution of the whole solids in SCC, thus including cement and cement substitutes, where $d_{\min}$=0.5 μm is employed. Since in this stage of the proposed mix-design method for (fiber reinforced) self-compacting concrete only the aggregates (and fibers, if applicable) are dealt with and the content of cement and cement substitutes is regarded as a part of the paste rheology optimization, it is believed that q=0.5, as for the Fuller and Fuller-like grading curves, should represent a reasonable choice.

Fibers, when applicable, are handled as an "equivalent spherical particle" fraction, with 100% passing fraction at an equivalent diameter, $d_{\text{eq-fibers}}$, defined through the specific surface area equivalence:

$$d_{\text{eq-fibers}} = \frac{3L_f}{1 + 2\frac{L_f}{d_f}} \frac{\gamma_{\text{fiber}}}{\gamma_{\text{aggregate}}} \tag{4}$$

where L_f and d_f are the length and diameter of the fibers, respectively, γ_{fiber} is the specific weight of fibers and $\gamma_{\text{aggregate}}$ is the weighted average specific weight of all the aggregates. It is worth remarking that L_f should be taken equal to the developed length in the case of non-straight fibers. Eq. (4) has been derived under the assumption that the surface area of the total amount of fibers added to the unit volume of concrete has to correspond to the surface area of an equal mass of spheres having the same (average) specific weight of aggregates.

As a matter of fact the content of fibers is specified as a percentage over the bulk volume of concrete. In order to include their contribution into the grading of the solid fraction, this volume percentage has to be related to the volume ratio of solids: the volume fractions of cement paste and of the solid particle skeleton have hence to be assessed at this stage. Their values are likely to affect the mass ratios of fine and coarse aggregates, for the optimization of the solid skeleton according

Table 1
Properties of cement and fly ashes

Chemical data	%
OPC type I (ASTM C150-04)	
Silicon dioxide (SiO_2)	20.1
Aluminum oxide (Al_2O_3)	4.9
Ferric oxide (Fe_2O_3)	2.8
Calcium oxide (CaO)	64.3
Magnesium oxide	2.5
Sulphur trioxide (SO_3)	2.4
Loss on ignition	1.55
Insoluble residue	0.25
Free lime	1.52
Tricalcium silicate (C_3S)	66
Tricalcium aluminate (C_3A)	8
Available alkali (equivalent Na_2O)	0.51
Blaine specific surface (m^2/kg)	352
% passing at #325 mesh	98.7
Density (kg/m^3)	3150
Fly ash class C (ASTM C 618)	
Silicon dioxide (SiO_2)	31.35
Aluminum oxide (Al_2O_3)	16.77
Ferric oxide (Fe_2O_3)	5.57
Calcium oxide (CaO)	23.26
Magnesium oxide	5.45
Sulphur trioxide (SO_3)	2.02
Loss on ignition	0.13
Moisture content	0.12
Sodium oxide Na_2O	2.07
Potassium oxide K_2O	0.31
Available alkali (equivalent Na_2O)	1.0
% passing at #325 mesh	87.2
Density (kg/m^3)	2740

Table 2
Summary of paste composition

Paste composition			
Volume % of cement (of solids)		70	
Volume % of fly ashes (of solids)		30	
w/b ratio (by weight)	0.32	0.36	0.4
Weight % superplasticizer (of solids)	0.35	0.45	0.55

to Eq. (1). Note that this is not the case for plain concrete. For the fiber-reinforced skeleton, the "average equivalent diameter of solid particles" can be expressed as:

$$d_{av} = \frac{\sum_i d_i m_i + d_{eq-fibers} m_{fibers}}{\sum_i m_i + m_{fibers}} \quad (5)$$

where d_i and m_i are defined as above with reference to Eq. (1), $d_{eq\text{-}fibers}$ is defined in Eq. (4), m_{fibers} is the mass of the fibers. The void ratio, V_{void}, of the graded solid fraction (including fine and coarse aggregates and fibers — if applicable — in the desired quantity) is measured according to ASTM C29/C29 M05 [33]. Once the paste content is also assessed, the average aggregate, or solid particle, spacing d_{ss}, for both plain and fiber-reinforced SCCs, can be calculated through Eq. (2).

3. Assessment of the mix-design model

3.1. Investigation one rheology

Taking advantage of previous investigations [8,9,34], a series of cement pastes was prepared, consisting of Type I Ordinary Portland Cement, Class C fly ash, water and a polycarboxylate based superplasticizer (SP). The properties of cement and fly ash are listed in Table 1, while Table 2 gives the details of the paste composition for the experimental program. Variables have been combined as shown in the test matrix in Fig. 2: three water–binder (w/b) ratios have been employed,

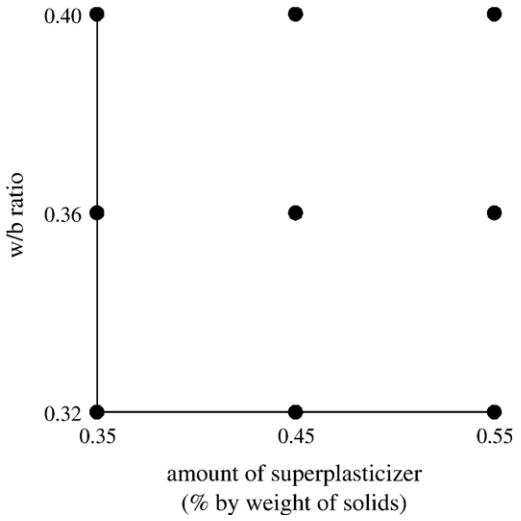

Fig. 2. Test design matrix for paste program.

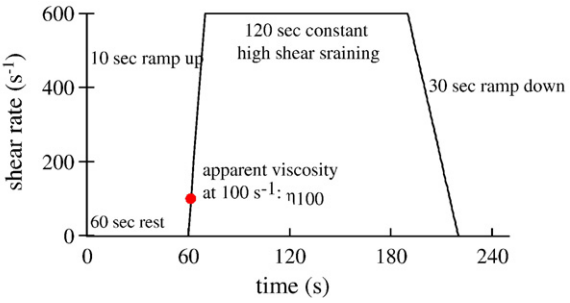

Fig. 3. Rheometric protocol for cement pastes.

namely 0.32, 0.36 and 0.40, and three different dosages of the SP, namely 0.35, 0.45 and 0.55% by weight of solids. The fly ash volume replacement ratio was kept constant at 30% in all the mixes. The SP dosages were chosen within the range suggested by the manufacturing company. The following mixing protocol was adopted: cement and fly ash were placed together with water and SP in a planetary mix and mixed for 1 min at low speed. After 1 min rest for scraping the sides of the bowl, the paste was further mixed for 1 min at high speed.

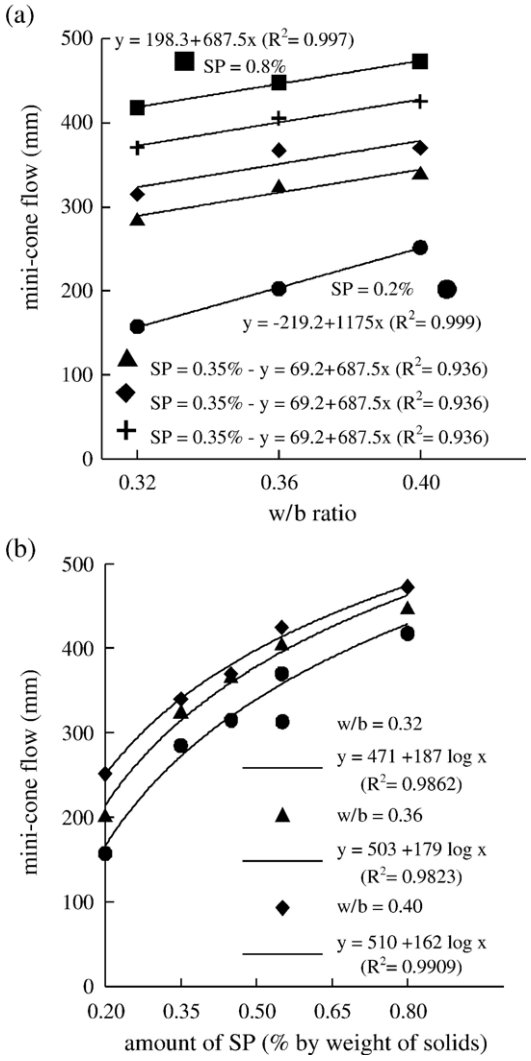

Fig. 4. Paste slump flow vs. w/b ratio (a) and SP amount (b).

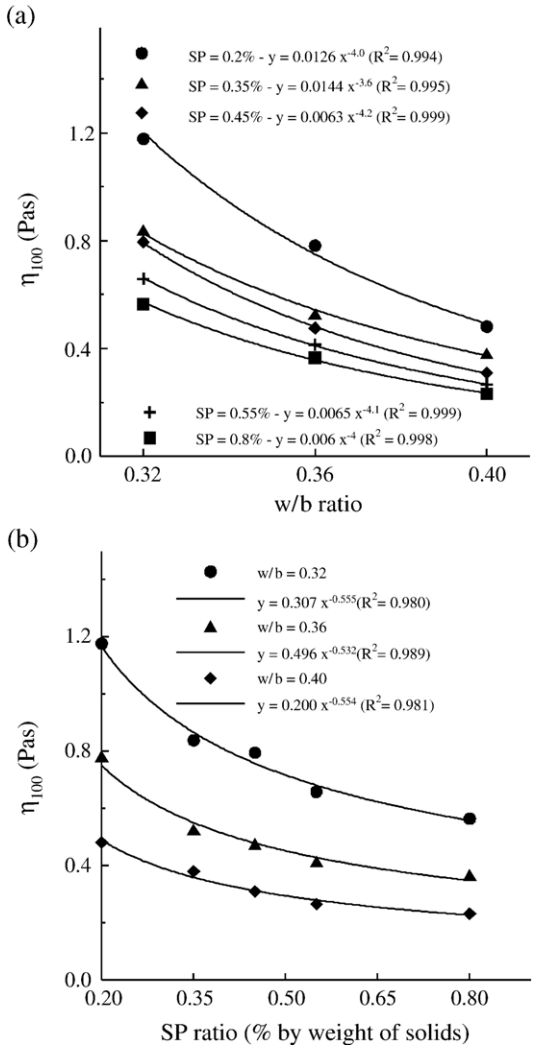

Fig. 5. Paste apparent viscosity η_{100} vs. w/b ratio (a) and SP amount (b).

The rheological properties of the paste were hence measured through the mini-cone-flow test and rheometer tests. For the mini-cone flow test, a frustum of cone, having lower and upper diameters of 100 mm and 70 mm respectively and a height equal to 50 mm, was employed. The mini-cone flow has been taken as the average diameter measured at four right-angle positions when the paste the frustum was filled with stopped flowing after vertically lifting the cone. The viscosity was measured through a BTT-Haake rheometer with a concentric cylinder configuration (0.8 mm gap between the cylinders), according to the same protocol adopted in [9], also sketched in Fig. 3. After the mini-cone flow test, the cement paste was transferred into the rheometer and, after 1 min rest, the shear rate was ramped up to 600 s^{-1}, over a 10 s interval. Then this high shear rate was held constant over a 120 s interval, and after it was linearly decreased down to zero in 30 s. Six measuring points per second were sampled along both the ascending and descending branches of the applied strain rate path while only one measure per second was taken along the constant shear rate branch. Consistently with [9], the apparent viscosity at an applied strain rate $\dot{\gamma}=100\ s^{-1}$ has been computed as the ratio to the strain rate of the shear stress measured on the ascending branch. The possibility for further investigating and assessing the rheological properties of the cement paste has been explored. A vane configuration of the rheometer has been also employed to measure the yield stress, applying a very low constant shear rate (0.01 rad/s — see [8]). The difficulty of such a procedure when applied to very fluid cement pastes, such as the ones formulated from SCCs, already pointed out [9] mainly with reference to the time required to attain the equilibrium condition, have been likewise faced in this work.

The trend of the measured mini-cone flow and apparent viscosity versus both the employed w/b ratios and amount of SP are shown in Figs. 4 and 5; for the SP dosage also weight ratios to solid equal to 0.2 and 0.8 (almost coincident with the boundaries of the recommended employment range) have been investigated in order to properly get the non-linear trend, if any, of the paste properties. It can be observed (Fig. 4a) that the mini-cone flow almost linearly increases with the water–binder ratio, at a rate that, except for very low dosages of SP, appears to be substantially independent of the SP content. The trend vs. the SP content for different values of the w/b ratio (Fig. 4b) appears to be well fitted by logarithmic curves: the influence of the

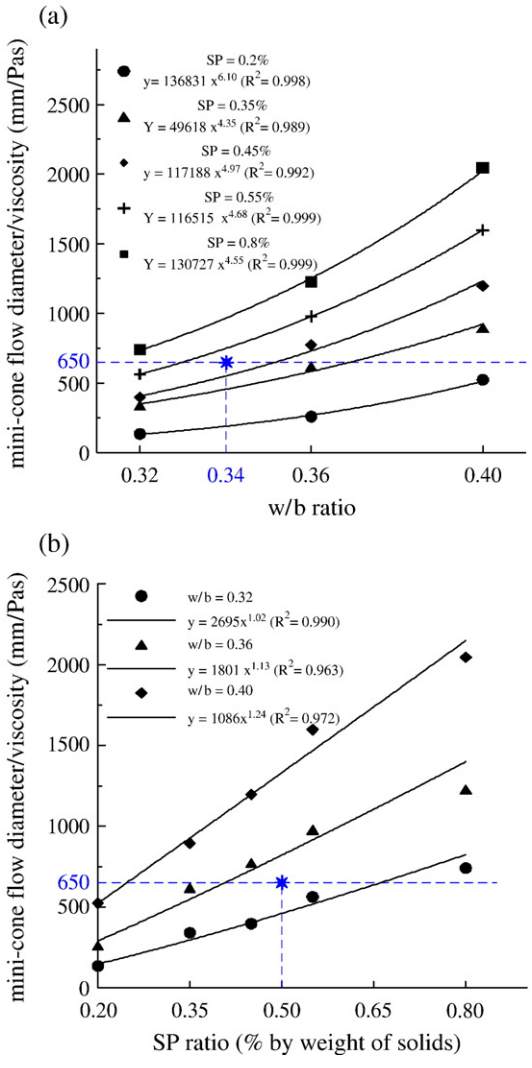

Fig. 6. Paste slump flow diameter/viscosity ratio vs. w/b ratio (a) and SP amount (b).

Table 3
Properties of aggregates

Sieve diameter (mm)	% passing	
	Coarse	Fine
12.5	100	100
9.5	100	100
4.75	13.4	99.8
2.36	3	89.6
1.18	2	71.3
0.600	–	50.3
0.300	–	18.4
0.150	–	4.1
0.075	–	1.1
0	0	0
Specific gravity (kg/m^3)	2650	2660
Absorption (%)	2.37	1.77

employed w/b ratios on the rate of variation of the mini-cone flow with the SP content appears to be small. This may suggest that the influence of the interaction between w/b ratio and SP content on the mini-cone flow diameter may be small. A power law trend of the measured apparent viscosity vs. both the w/b ratio (Fig. 5a) and the amount of SP (Fig. 5b) has been detected: the higher is the SP amount (w/b ratio), the lower is the effect of the w/b ratio (SP amount respectively), thus suggesting a stronger interaction of w/b and SP content on the viscosity than on the flow diameter (yield stress).

In the framework of the rheological paste model [9], the ratio between the paste mini-cone flow diameter and apparent viscosity vs. both the water/binder ratio and the SP content has been also plotted (Fig. 6). The trend is in accordance with the statements made earlier when the mini-cone flow diameter and viscosity were separately analyzed: the computed ratio increases with the water/binder ratio (SP dosage) at a higher rate with higher SP content (w/b ratio).

3.2. Optimization of the solid skeleton grading: plain and steel fiber-reinforced concrete

Parallel to the rheological characterization of the paste, the optimal grading of the solid skeleton was pursued. Particle size

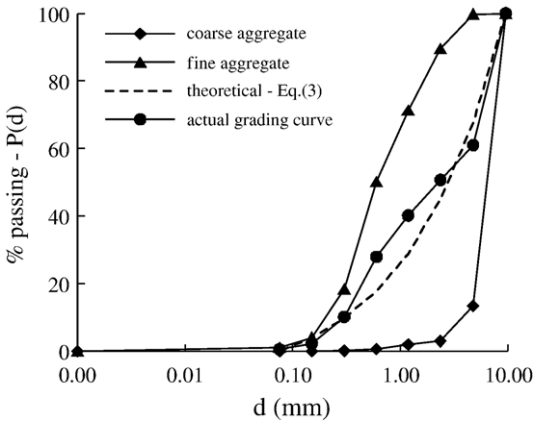

Fig. 7. Particle size distribution and grading curve of the aggregate skeleton for plain concrete.

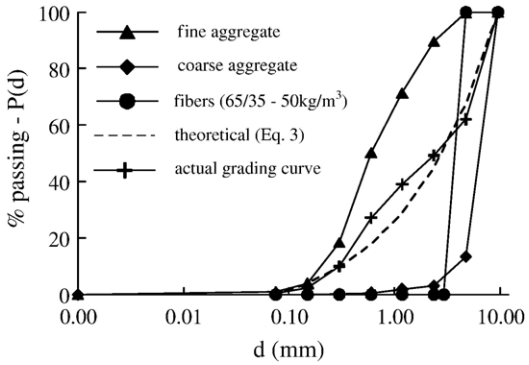

Fig. 8. Example of grading of fiber-reinforced solid skeleton.

distribution, specific gravity and absorption of the employed fine and coarse aggregates were determined, according to ASTM C136 [29], ASTM C127 and ASTM C128 [35,36] respectively. The results are summarized in Table 3, and, for the particle size distribution, shown in the usual log scale in Fig. 7. For plain concrete the optimization of the aggregate skeleton according to Eq. (3) led to a coarse to total aggregate mass ratio equal to 0.449, to which the grading curve also shown in Fig. 7 and an average aggregate diameter d_{av}=3.540 mm correspond (Eq. (1)). A void ratio equal to 21.49% was measured for such an aggregate skeleton.

The application of the proposed approach to solid skeleton grading in the case of (steel) fiber-reinforced concrete has been attempted with fibers type Dramix 65/35, which have an aspect ratio equal to 65 and a length of 35 mm. As explained in Section 2, in the grading of solid skeleton fibers are treated as an equivalent spherical particle, with 100% passing fraction at a sieve opening equal to the diameter d_{eq}, computed according to the equivalent specific surface concept (Eq. (4): in the case of the fibers herein employed this turns out equal to 2.37 mm.

The quantity of fibers is usually specified with reference to the bulk concrete volume: once referred to the actual content of solid particles (fine and coarse aggregates + fibers) through the previous definition of their whole volume fraction (or, equivalently, through the definition of the cement paste volume fraction), it stands as a constraint in the grading of the solid skeleton. For the chosen dosage of 50 kg of fibers per cubic meter of concrete, employed in this first stage of the investigation, solid skeleton grading with the coarse, fine and fiber equivalent aggregate fractions has been optimized for different fiber to total aggregate ratios, corresponding to paste volume ratios ranging between 0.32 and 0.44. As in the case of

Table 4
Fiber and aggregated grading and void ratio in fiber-reinforced solid skeletons

Fiber data		d_{eq} (mm)	V_p	Solid skeleton (% by mass)			d_{av} (mm)	V_{void}
Type	Quantity (kg/m^3)			% mass fibers	% mass coarse aggr.	% mass fine aggr.		
Dramix 65/35	50	2.37	0.32	2.77	43.70	53.53	3.541	22.52
			0.36	2.95	43.60	53.45	3.541	24.03
			0.40	3.14	43.53	53.33	3.541	22.58
			0.44	3.37	43.42	53.21	3.541	24.24

Table 5
Mix design for plain and fiber-reinforced concrete mixes and fresh state test results

Mix	w/b	SP (% solids)	d_{ss} (mm)	Plain concrete				Comment
				V_p	Flow diameter (mm)	T_{50} (s)	VSI	
1	0.36	0.55	0.272	0.32	615	6	0.5	Higher T_{50}
2	0.32	0.35	0.272	0.32	//	//	//	No slump loss at all!
3	0.4	0.45	0.272	0.32	560	5	0	Poor deformability
4	0.36	0.45	0.361	0.36	710	3	1	Excellent flow and stability
5	0.32	0.55	0.361	0.36	725	5	1.5	Good flow
6	0.40	0.35	0.361	0.36	650	2	2	Good flow but some segregation
7	0.36	0.35	0.459	0.40	725	2	2	Segregation
8	0.32	0.45	0.459	0.40	800	1	3	Severe segregation
9	0.40	0.55	0.459	0.40	750	3	1.5	excellent flow and stability
				SFRC				
1FRC	0.36	0.55	0.272	0.327	590	5	0.5	Poor deformability
2FRC	0.32	0.35	0.272	0.327	//	//	//	No slump loss at all!
3FRC	0.4	0.45	0.272	0.327	550	4	0	Poor deformability
4FRC	0.36	0.45	0.361	0.366	690	3	1	Excellent flow and stability
5FRC	0.32	0.55	0.361	0.366	705	5	1	Good flow and stability
6FRC	0.40	0.35	0.361	0.366	640	2	2	Good flow with some segregation
7FRC	0.36	0.35	0.459	0.405	700	2	2.5	Segregation
8FRC	0.32	0.45	0.459	0.405	800	1	3	Severe segregation
9FRC	0.40	0.55	0.459	0.405	740	3	1.5	Excellent flow

plain concrete, Eq. (3) was employed as the optimal theoretical grading curve (Fig. 8). The trend of fine and coarse aggregate mass fractions with increasing volume ratio of cement paste is summarized in Table 4. It is worth emphasizing that this solid skeleton grading procedure yielded a constant value of the average equivalent aggregate diameter (Eqs. (1) and (4)), irrespective of the paste volume ratios. The void ratios for the thus graded combinations of fine and coarse aggregates and fibers have been also measured according to [33] (Table 4). A scant influence of the content of fibers has been detected. For this reasons, for further applications dealing with the design of fiber-reinforced self-compacting concretes, a constant value equal to the average of the experimentally measured ones has been employed (V_{void}=23.29%). The close values of void ratios measured for optimized solid skeleton with and without fibers are likely to confirm the reliability of the proposed procedure for grading of fiber-reinforced solid skeletons.

3.3. Concrete proportioning and testing for self-compactability

The final stage in the application of the rheological paste model for the design of plain and fiber-reinforced self-compacting concretes consists in combining a cement paste with given rheological properties with the particles of solid skeleton, suitably graded according the chosen optimum criterion. At this stage the paste volume ratio becomes another variable in the mix-design procedure. The paste volume ratio governs the average spacing between solid particles and, as a consequence, the required rheological properties of the paste to obtain a concrete with the desired flowability and stability characteristics. In the present work, for plain concrete the following paste volume ratios have been employed: V_p=0.32, 0.36 and 0.40. They correspond, for solid skeleton graded as in Fig. 6 (coarse/fine ratio=0.815; void ratio=21.94%), to an average aggregate spacing respectively equal to 0.272, 0.360 and 0.459 mm. For fiber-reinforced mixes in order to keep, for the sake of consistency, the same values of average aggregate spacing, the slightly different measured void ratio led to consequently modified paste volumes (see Tables 5 and 6, for the solid skeleton grading).

For the assessment of the model, nine plain and nine fiber-reinforced concretes have been cast, the composition of which is dictated by the paste volume ratio, water/binder ratio and superplasticizer content in the paste. The values of these three independent variables have been combined according to a 3^{3-1} fractional factorial replication, as detailed in Table 5.

The following mixing protocol was adopted: first aggregates, cement and fly ashes were placed in a Hobart planetary mixer and dry-mixed at low speed for 3 min. Then, 75% of the water was added and mixed further for 3 min at low speed. After 1 min rest for scraping the sides of the mixing bowl the remaining water, superplasticizer were added and further mixed for 1 min at low speed, during which fibers, if applicable, were added, and finally 3 further min mixing at high speed was allowed. The content of water actually added to the mix was adjusted for half the absorption capacity of aggregates, always employed in an oven dry conditions.

The key feature of the rheological paste model stands in establishing suitable correlation between the rheological

Table 6
Solid skeleton grading for fiber-reinforced concretes

Fibers		d_p (mm)	V_p	Solid skeleton (% by mass)			Average particle size (mm)	V_{void}	d_{ss} (mm)
Type	Quantity (kg/m^3)			% mass fibers	% mass coarse aggr.	% mass fine aggr.			
Dramix 65/35	50	2.37	0.327	2.75	43.70	53.55	3.54	23.3	0.272
			0.366	2.91	43.62	53.46	3.54		0.361
			0.405	3.10	43.54	53.33	3.54		0.460

properties of the paste, the average size and spacing of the solid skeleton particles in concrete, and the fresh state behavior of the concrete itself, so that the anticipated fluidity and rheological stability characteristics can be achieved. To this purpose slump flow tests have been performed, measuring both the diameter of the concrete spread at the end of the test, which may be correlated to the yield stress [14], and the time needed to reach a 500 mm diameter spread, T_{50}, which is thought to be an indicator of the concrete viscosity [11] (see Table 5 for results). The following acceptance requirements have been set:

- flow diameter (measured to the nearest mm): between 600 and 750 mm
- T_{50} (measured to the nearest second): between 2 and 5 s

values outside the prescribed ranges represented concrete which has a greater potential for static and dynamic segregation or poor deformability.

The "visual segregation index" VSI (ranging between 0 — no evidence of segregation — and 3 — strong segregation — see [11]) was used to evaluate the segregation resistance of the concrete, as this was the only "simple" method available to the authors for both plain and fiber-reinforced mixes. A VSI equal or larger than 2 has been regarded as unacceptable. Penetration probes and devices [2,19], may be questionable in the case of fiber-reinforced concretes and for this reason they have not been used in this work. Further tests on segregation have been made for fiber-reinforced concretes. Fiber dispersion was first of all evaluated from slump flow test: fibers in the outer ring (outside 500 mm) and in the inner circular part (inside 200 mm) of the slump flow have been separated by washing and their weight ratio to the bulk concrete, determined to the nearest 0.1 g after wiping them, has been measured. The dispersion of fibers was also checked along the height of cylinders 200 mm high and with a 100 mm diameter (two per each mix), cut along a diameter plane after being tested for compression strength [37]. Results and related "acceptance criteria" will be discussed in the forthcoming pages.

With reference to passing ability, it has to be underlined that related testing devices prescribed by international standards (L-box, U-box, and J-ring) actually provide obstacle spacing which is too narrow for the length of the fibers employed in this study (35 mm). These devices were developed based on common congested reinforcement patterns in plain concrete structures and calibrated on a maximum aggregated size recommended for SCC equal to 20 mm (actually the spacing ranges between twice and three times that maximum particle diameter). A calibration based on the length of the fibers would lead to gauge spacing which is meaningless for plain concrete mixes (more than five times the recommended maximum aggregate size) and not easily matching with the size of the devices as currently prescribed by standards. It has to be furthermore taken into account that one of the reasons to use fibers could be the reduction of reinforcement in congested areas. For such a case the issue of passing ability may be not so crucial when fiber-reinforced self-compacting mixes are dealt with. This problem may by the way deserve further careful investigation and has not been addressed in this work.

The basics of the model used for proportioning fiber-reinforced self-compacting concretes has been hence assessed through the analysis of the whole set of the above mentioned results.

3.3.1. Paste slump flow and concrete deformability

The results of slump flow tests on concretes, both in terms of flow diameter and T_{50}, have been plotted versus the rheological properties of the cement paste. The mini-cone flow diameter and viscosity of the paste have been referred to the density difference between the solid skeleton and the paste. Data have been grouped for plain and fiber-reinforced concretes together and for each of the three values of the average aggregate spacing d_{ss} considered in the mix design.

A strong correlation is observed between the slump flow diameter of concrete and the mini-cone flow diameter of the cement paste (Fig. 9). Data from plain and fiber-reinforced concretes, for the same value of d_{ss}, appear to be consistent, thus proving the reliability of the approach proposed for taking into account the presence of fibers in the optimum grading of the solid skeleton. Minimum and maximum values of the mini-cone flow diameter of cement paste required for the concrete slump flow to fall within the prescribed boundaries (600–750 mm) can be easily computed from the equations of the trend-lines fitting experimental data (Fig. 9). As expected, the more dilute is the suspension (higher average aggregate spacing d_{ss}), the lower are both those values, because a lower flow diameter (higher yield stress) is required to fulfil the deformability requirements. From the minimum and maximum values computed as above, the model trend lines for the paste mini-cone flow diameter can be derived (Fig. 10). Experimental data have been plotted, as a function of the average aggregate spacing, together with the model boundary lines for mini-cone flow of cement paste, derived on the basis of values computed as in Fig. 9. It can be

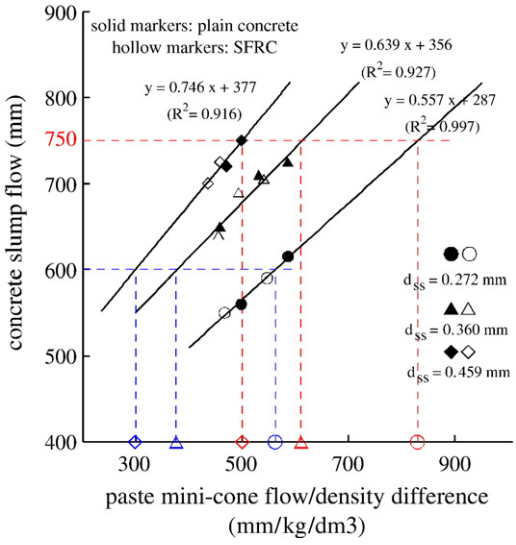

Fig. 9. Slump flow of concrete vs. ratio between the mini-cone flow of cement paste and the density difference between solids and paste.

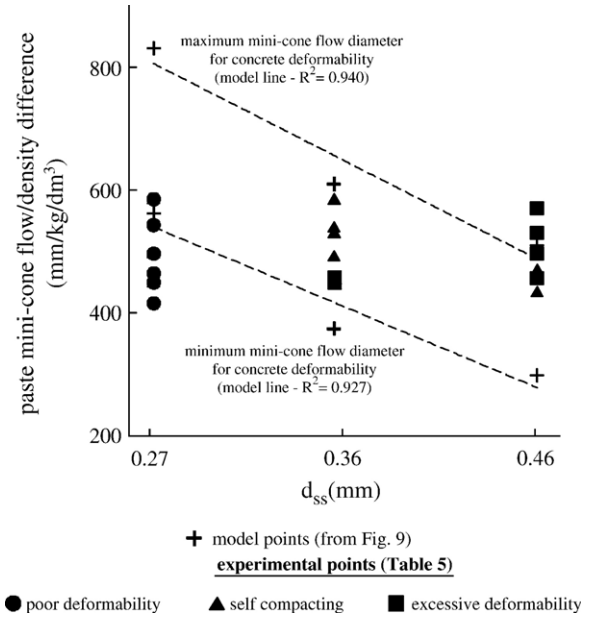

Fig. 10. Mini-cone flow diameter of paste and aggregate spacing (model lines and experimental data).

observed (see Table 5) that all data points falling below the minimum mini-cone flow model line represent a concrete with poor deformability and, likewise, all data points beyond the maximum mini-cone flow line actually correspond to concrete which exhibited excessive spread. By the way not all the points falling within the boundaries satisfy requirements for self-compacting concrete (Fig. 10). Thus, the criterion based on the paste flow diameter alone is not sufficient for a thorough assessment of self-compactability.

3.3.2. Paste viscosity and concrete fluidity

The time employed by fluid concrete to reach a 500 mm diameter spread in the slump flow test, T_{50}, has been tentatively connected to the viscosity of the cement paste (η_{100}, see above for details). Increasing the paste viscosity increases the value of T_{50}, at a decreasing rate for higher average aggregate spacing (Fig. 11). The trend seems to be similar for both plain and fiber-reinforced concrete. As for the flow diameter of cement paste, minimum and maximum values of the cement paste viscosity can be derived from trend lines fitting experimental data, so that the measured T_{50} falls within the above mentioned allowable boundaries (Fig. 11). In order to thoroughly assess the requirements on minimum and maximum viscosity of cement paste, this information has to be completed with data on the resistance to segregation.

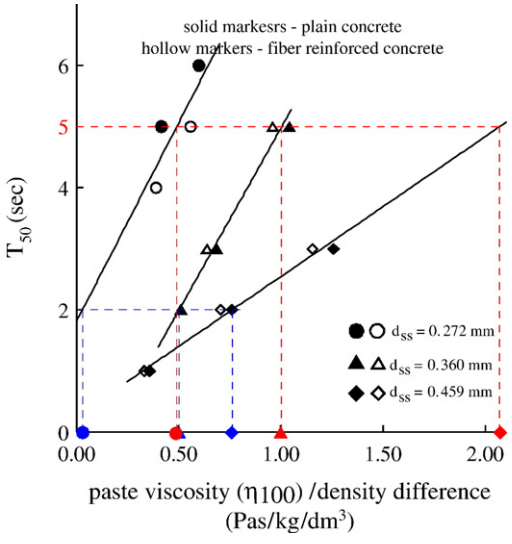

Fig. 11. T_{50} vs. ratio between the viscosity of cement paste and the density difference between solids and paste.

3.3.3. Paste viscosity and resistance to segregation

Besides the assignment of a Visual Segregation Index (VSI) to each mix (Table 5), for fiber-reinforced concretes the issue of segregation resistance has been also checked with reference to the dispersion of fibers in the outer crown (outside 500 mm diameter) and in the inner circle (inside the 200 mm diameter) of

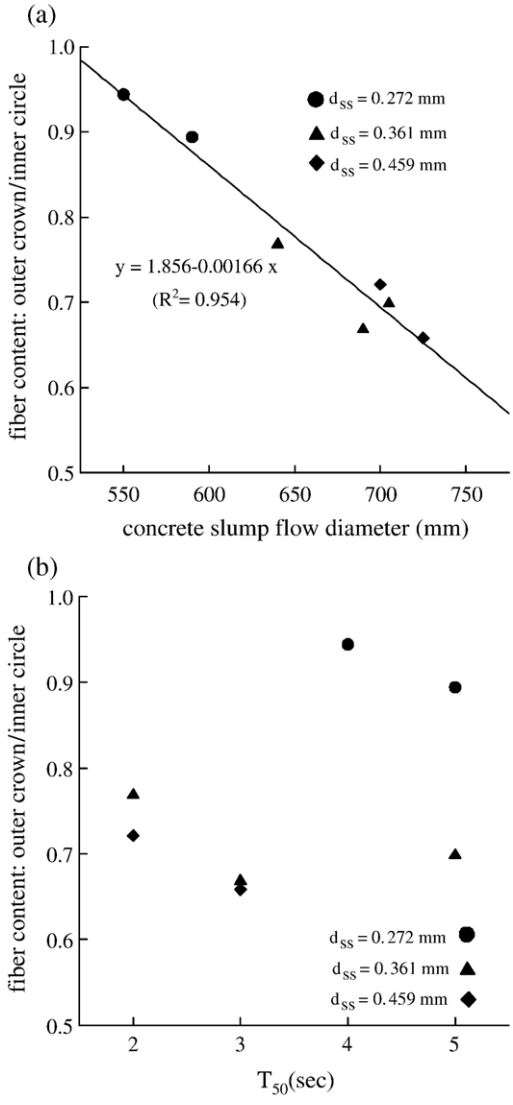

Fig. 12. Fiber dispersion ratio (outer/inner) vs. concrete slump flow (a) and T_{50} (b).

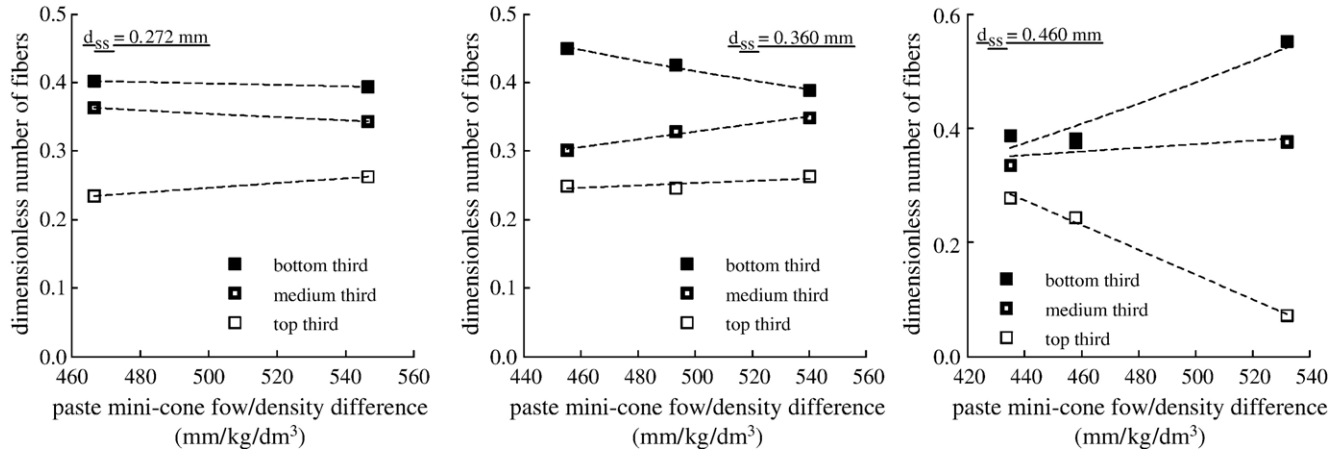

Fig. 13. Dimensionless number of fibers along the height of cylinder specimens vs. paste slump flow diameter for different average aggregate spacing d_{ss}.

the slump flow. The measured values of the fiber mass ratio in the outer crown, relative to that in the inner circle, show a good trend vs. the concrete slump flow (Fig. 12a), while hardly any dependence could be sought neither versus T_{50} (Fig. 12b) or versus the mini-cone flow and viscosity of the cement paste.

A check of the fiber distribution along the height of 100 × 200 mm (diameter × height) cylinders was hence performed. To this purpose cylinders, after tested for compression strength, were cut along a diameter plane. The number of fibers in the top, middle and bottom third of a diameter plane of the cylinders, relative to the total number of fibers, has been interestingly correlated, also as a function of the average aggregate spacing d_{ss}, to the rheological properties of cement paste (Figs. 13 and 14).

For smaller average aggregate spacing the distribution of fibers along the specimen height hardly depends on the rheological properties of the cement paste, while for larger values of the spacing fibers clearly tend to settle downward. The more fluid and less viscous is the cement paste (higher mini-cone flow diameter or lower viscosity) and the more dilute the suspension (higher d_{ss}), the stronger is the tendency of fibers to segregate, even if the dependence on the mini-cone flow diameter appears to be somewhat controversial for lower d_{ss} (see Fig. 13b where for a higher mini-cone flow a more uniform dispersion of fibers has been measured). It is furthermore worth noting that, even for the more densely suspended mixes as well as for the less fluid and more viscous pastes, the dimensionless fiber number in the bottom third of the cylinder hardly falls below 0.40, whereas, on the other hand, values always below 0.30 have been measured in the top third. As a limit, in this work a dimensionless number of fibers in the top third not less than half in the medium and bottom ones have been set. From the trend lines fitting data of the dimensionless number of fibers vs. the viscosity of the cement paste, based on the above said acceptance criterion, minimum viscosity values to avoid segregation can be computed, which turned out to be more stringent than the minimum ones computed previously on the basis of concrete fluidity (T_{50}).

Model lines for cement paste viscosity can be hence derived from both minimum values, computed with reference to resistance to segregation, and maximum ones, as derived in the previous subsection with reference to concrete fluidity (T_{50}—Fig. 15). Plotting the experimental data together with the model

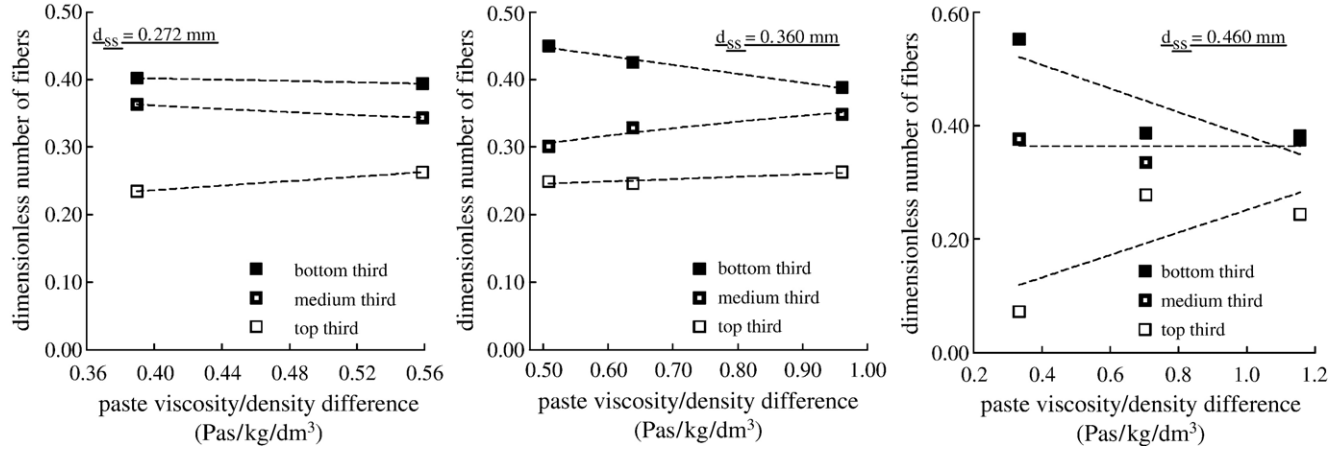

Fig. 14. Dimensionless number of fibers along the height of cylinder specimens vs. paste viscosity for different average aggregate spacing d_{ss}.

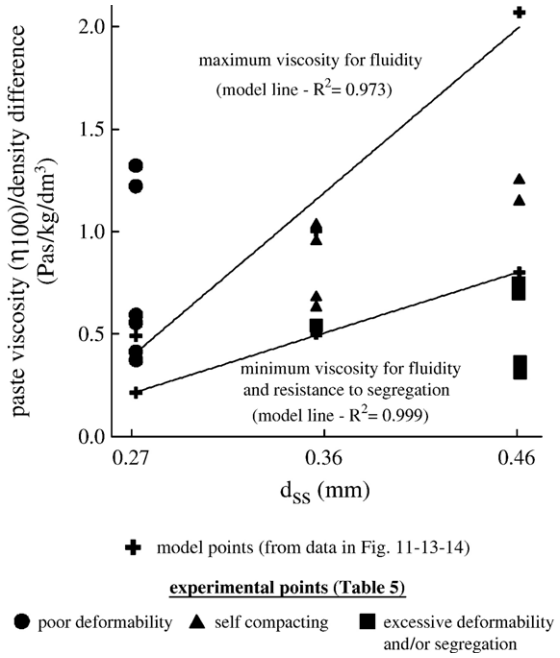

Fig. 15. Minimum paste viscosity and aggregate spacing (model line and experimental data).

trend lines, also as a function of the average aggregate spacing (Fig. 15), it appears that the more dilute is the suspension (higher d_{ss}) the higher the minimum viscosity of cement paste required to avoid segregation. It can be also observed that all data points falling below the minimum viscosity line represent a concrete featured by segregation and/or excessive fluidity, as well as all the points falling above the trend line for maximum viscosity represent a concrete with poor deformability. Still not all the points between the minimum and maximum viscosity model lines represent a self-consolidating concrete.

3.3.4. Optimum flow diameter to viscosity ratio of cement paste for self-compactability

As indicated earlier, neither the paste flow diameter nor the paste viscosity is a sufficient independent parameter to describe SCC. In accordance with the suggestion given in Ref. [9], these two parameters were combined as a ratio of mini-cone flow diameter and viscosity. From the limiting values of each of these parameters, regression lines representing upper and lower limits were drawn (Figs. 10 and 15). From these lines, the limiting curves representing the ratios were calculated and drawn in Fig. 16. The consistency of this approach clearly appears when the experimental data points for plain and fiber-reinforced concrete are plotted as a function of the average aggregate spacing together with model lines (Fig. 16). The position of data points is always consistent with the "physical" significance of the model lines that divide the plane into poor deformability, self-compactability and segregation regions. Model lines clearly show as a minimum and a maximum value of the flow diameter to viscosity ratio of the cement paste are required in order to guarantee sufficient deformability of concrete and avoid segregation respectively. Both these minimum and maximum values decrease with the average aggregate spacing, indicating that a lower flow diameter and a higher viscosity of the paste are required for more dilute suspensions to fulfill the requirements on deformability and rheological stability for self-consolidating concrete. It is also interesting to underline that for higher average aggregate spacing, which means for more dilute suspensions of solid particles in the fluid cement paste, a wider range of possibilities, with reference to paste rheological properties, seems to be available for designing a self-compacting concrete. This aspect, which is consistent with findings by Bui et al. [9], may deserve further investigation with reference to different types of aggregates and fibers etc.

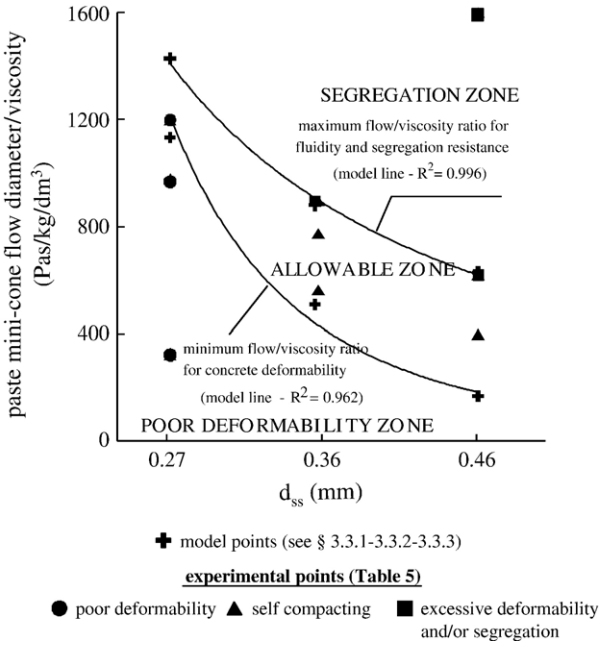

Fig. 16. Paste slump flow diameter to viscosity ratio (model lines and experimental data).

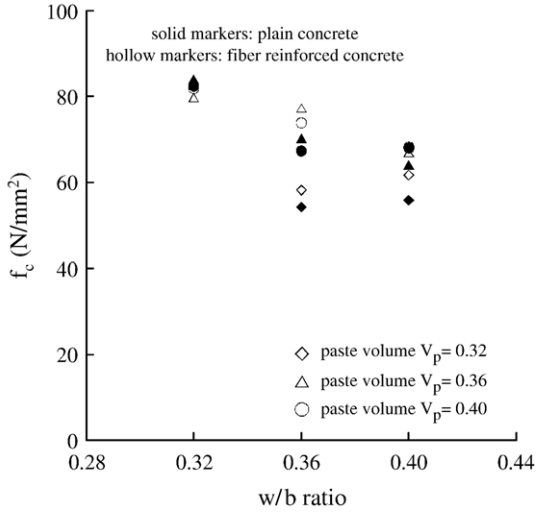

Fig. 17. 56-day cylinder compressive strength vs. w/b ratio.

3.3.5. Compressive strength

The assessment of the model has been completed through compression strength tests performed on cylinder specimens 200 mm high and with a diameter equal to 100 mm (two per each mix) after 56 days curing in moist room. The results confirm the well known trends vs. the w/b ratio (Fig. 17) and further prove the reliability of the mix-design approach, consistent values having been obtained for "equivalent" plain and fiber-reinforced mixes.

4. Application of the model: mix-design of self-compacting SFRC

The concepts of optimum limiting values of flow–viscosity ratio, developed from the analysis of results and graphically summarized in Fig. 16, can be usefully employed for the design of self-compacting fiber-reinforced concretes, according to the process which has been summarized in the flow chart in Fig. 18.

As an application of the developed model, three mixes have been designed to investigate on connections between fresh state properties, fiber dispersion and hardened state properties in steel fiber-reinforced concretes. The three mixes, all containing 50 kg/m^3 steel fibers type Dramix 65/35, are respectively featured by poor deformability (mix A), "good" self-compacting properties (mix B), and the last by poor resistance to segregation (mix C). Employing the design graph of Fig. 19, the task has been accomplished by employing the same cement paste, featured by a chosen value of the flow diameter to viscosity ratio equal to 650, in the same three different volume ratios as before (V_p=0.32, 0.36, and 0.40), thus obtaining three different "degrees of suspension" of the solid skeleton (d_{ss}=0.272, 0.360 and 0.460 mm respectively). The design target points are also shown in Fig. 19: they fall well within the self-flow zone for d_{ss}=0.360 mm (mix B) and slightly outside it, on the segregation side, for d_{ss}=0.460 mm

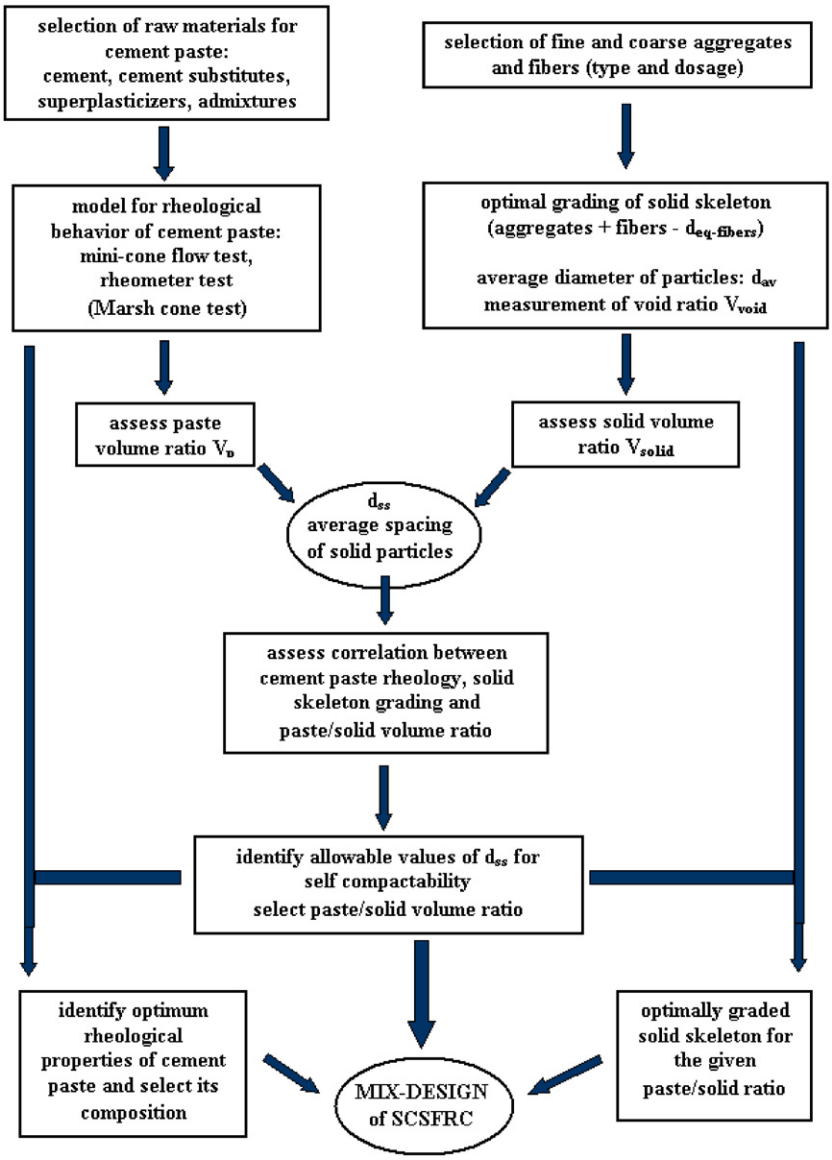

Fig. 18. Flow chart for mix design of SCSFRC.

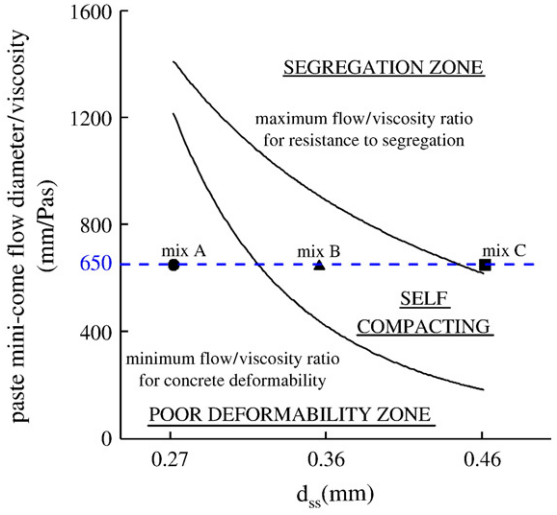

Fig. 19. Experimental points (design application) and minimum/maximum flow–viscosity ratio model lines.

(mix C), while being well below the poor deformability threshold for $d_{ss}=0.272$ mm (mix A).

From the model equations obtained in the Section 3.1 (see also Fig. 6) the composition of cement paste has been derived, namely corresponding to a w/b ratio equal to 0.34 and an SP content equal to 0.5% by weight of solids; the fly ash replacement ratio has been kept equal to 30% by volume. For an estimated density difference between the solid skeleton and the cement paste of 0.7 kg/dm^3, and according to the previously developed paste rheology model, a slump flow diameter of 360 mm and a viscosity equal to 0.56 Pas are expected. The predictions have been excellently confirmed by measured values of 370 mm and 0.57 Pas respectively (slump flow to viscosity ratio equal to 649).

The solid skeleton grading for the three concretes is detailed in Table 7, together with flow diameter and T_{50} measured from slump flow tests and the assigned VSI. For the slump flow diameter, the given value corresponds to the average of three nominally equivalent measures; all three measures have been reported for T_{50} and the VSI. These data clearly show as the above mentioned target of designing three fiber-reinforced mixes with different fresh state behavior has been accomplished and hence stand as a proof of the reliability of the proposed mix-design approach for self-compacting fiber-reinforced concrete.

Table 7
Mix-design and measured flow properties of SFRCs designed from Fig. 18 (all mixes contain 50 kg/m^3 fiber type Dramix 65/35)

Mix	V_p	d_{ss}	Solid skeleton (% by mass)			Flow diameter (mm)	T_{50} (s)	VSI
			% mass fibers	% mass coarse aggr.	% mass fine aggr.	exp.	exp.	
A	0.327	0.272	2.747	43.70	53.55	360	=	0
B	0.366	0.360	2.913	43.62	53.46	650	4;4;3	1.5,1.5,1
C	0.405	0.460	3.100	43.54	53.33	780	2;2;1	3,3,3

Table 8
Void ratio in solid skeletons with different types and ratios of fiber reinforcement

Fiber data		d_{eq} (mm)	V_p	Solid skeleton (% by mass)			d_{av} (mm)	V_{void}
Type	Quantity (kg/m^3)			% mass fibers	% mass coarse aggr.	% mass fine aggr.		
Dramix 65/35	80	2.37	0.32	4.30	42.99	52.70	3.54	22.68
			0.36	4.57	42.88	52.56	3.54	21.17
			0.40	4.86	42.74	52.40	3.54	24.78
Dramix 65/60	50	4.08	0.32	2.72	43.11	54.17	3.53	20.85
			0.36	2.89	43.01	54.10	3.53	21.64
			0.40	3.08	42.90	54.03	3.53	21.46
Dramix 65/35 65/60	25+25	2.37 4.08	0.32 01.36 0.40	2.72 2.89 3.08	43.41 43.33 43.23	53.87 53.79 53.69	3.53 3.53 3.53	22.11 21.82 22.31

4.1. Effect of fiber volume fraction and fiber type

As a further a check, the role of fiber dosage and fiber type has been investigated. Three different cases have been selected: a fiber-reinforced concrete with 80 kg/m^3 fibers type Dramix 65/35 (mix D), a second one containing 50 kg/m^3 fibers type Dramix 65/60 (mix E) and a concrete with a hybrid fiber reinforcement consisting of 25 kg/m^3 fibers Dramix 65/35 and 25 kg/m^3 fibers Dramix 65/60 (mix F). The void ratios for the solid skeleton with the different types and ratios of fiber reinforcement have been first measured (Table 8). The scant variation of the measured values and their close proximity to the ones previously measured for unreinforced skeletons and for the case of 50 kg/m^3 of fibers Dramix 65/35 stand as a further confirmation of the reliable method to include fibers in solid skeleton optimization. An average value has been hence assumed in the mix design, independently on the chosen paste volume ratio. The values of the computed average aggregate diameter allow for a consistent comparison of the results and for a thorough assessment of the model predictions.

The same paste has been employed as detailed for concretes in the previous sub-section, always in a volume ratio such to have an average aggregate spacing equal to 0.360 mm. The mix composition of the three mixes is hence detailed in Table 9, together with the measured slump flow diameter and T_{50} values and the assigned VSI.

The data provide a further proof of the versatile reliability of the model when applied to the mix design of concretes, even with different quantities and types of fiber reinforcement (the case of longer fibers may deserve further investigation). An

Table 9
Mix-design and measured flow properties of SFRCs designed from Figs. 18 and 19: influence of different types and ratios of fiber reinforcement

Mix	Fiber		V_p	Solid skeleton (% by mass)			Flow diameter (mm)	T_{50} (s)	VSI
	Type	kg/m^3		% mass fibers	% mass coarse aggr.	% mass fine aggr.			
D	65/35	80	0.364	4.59	42.86	52.54	635	4	1
E	65/60	50	0.358	2.88	43.02	54.11	595	4/5	1
F	65/35	25	0.361	2.89	43.32	53.79	655	4/5	1
	65/60	25							

Fig. 20. Slump flow for SCSFRC mix D.

example of the slump flow for mix D is shown in Fig. 20: the size, compactness and roundness of its shape clearly show the accomplished target of designing a self-compacting steel-fiber reinforced concrete.

5. Conclusions

A simple method for mix design of self-consolidating fiber-reinforced concretes has been presented in this work and assessed, also through comparison with analogously designed plain self-consolidating concretes. The proposed method includes the fibers in the optimization of the solid skeleton through the concept of the "equivalent specific surface diameter". Optimization of rheological properties of cement paste and the appropriate choice of its volume ratio stand as further keys of the method. The model proved to be an efficient tool for designing fiber-reinforced concrete mixtures with selected fresh state properties, employing different ratios and types of steel fiber reinforcement. Further developments and application of the model with reference to differently graded aggregates, types and volume ratios of fiber reinforcement (even non-metallic ones) stand as a forthcoming extension of this work.

As a further prosecution of the work, the investigation on connections between fresh state properties, fiber dispersion and mechanical properties of fiber-reinforced cement composites is on going. An omni-comprehensive approach to the problem would allow to design the material and the casting process "tailored" to the dedicated structural applications. The possibility of controlling the homogeneity of fiber dispersion, for a reliable structural performance, and even governing their orientation, through the flow direction of fluid concrete, according to the anticipated prevalent stress patterns inside the structural element when in service, would represent the acme of the whole process.

Acknowledgments

This work has been performed during a visiting scholarship period spent by the first author at ACBM, Northwestern University, in the framework of a Fulbright Program, whose support is gratefully acknowledged.

References

[1] V. Corinaldesi, G. Moriconi, Durable fiber reinforced self-compacting concrete, Cement and Concrete Research 34 (2004) 249–254.
[2] SCC, in: S.P. Shah (Ed.), Proceedings of the 2nd North American Conference on the Design and Use of Self Consolidating Concrete (SCC) and the 4th International RILEM Symposium on Self-Compacting Concrete, Hanley Wood Pub., Addison IL, 2005.
[3] N. Su, K.C. Hsu, H.W. Chai, A simple mix-design method for self compacting concrete, Cement and Concrete Research 31 (2001) 1799–1807.
[4] H.J.H. Brouwers, H.J. Radix, Self compacting concrete: theoretical and experimental study, Cement and Concrete Research 35 (2005) 2116–2136.
[5] H. Okamura, Self compacting high performance concrete, Concrete International 19 (7) (1997) 50–54.
[6] F. De Larrard, Concrete Mixture Proportioning. A Scientific Approach, E&FN Spoon, 1999.
[7] R.J. Flatt, Towards a prediction of superplasticized concrete rheology, Materials and Structures 37 (2004) 289–300.
[8] A.W. Saak, H.M. Jennings, S.P. Shah, New methodology for designing self-compacting concrete, ACI Materials Journal 98 (6) (2001) 429–439.
[9] V.K. Bui, J. Akkaya, S.P. Shah, Rheological model for self-consolidating concrete, ACI Materials Journal 99 (6) (2002) 549–559.
[10] K.H. Khayat, A. Ghezal, M.S. Hadriche, Factorial design models for proportioning self-consolidating concrete, Materials and Structures 32 (1999) 679–686.
[11] K.H. Khayat, A. Ghezal, M.S. Hadriche, Utility of statistical models in proportioning self consolidating concrete, Materials and Structures 33 (2000) 338–344.
[12] K.H. Khayat, Y. Roussel, Testing and performance of self consolidating concrete, Materials and Structures 33 (2000) 391–397.
[13] K.H. Khayat, J. Assad, J. Daczko, Comparison of field oriented test methods to assess dynamic stability of self consolidating concrete, ACI Materials Journal 101 (2) (2004) 168–176.
[14] J. Assaad, K.H. Khayat, J. Daczko, Evaluation of static stability of self-consolidating concrete, ACI Materials Journal 101 (3) (2004) 207–215.
[15] S.D. Hwang, K.H. Khayat, O. Bonneau, Performance-based specifications of self consolidating concrete used in structural applications, ACI Materials Journal 103 (2) (2006) 121–129.
[16] A.W. Saak, H.M. Jennings, S.P. Shah, A generalized approach for the determination of yield stress by slump and slump flow, Cement and Concrete Research 34 (2004) 363–371.
[17] N. Roussel, Correlation between yield stress and slump: comparison between numerical simulations and concrete rheometers results, Materials and Structures 39 (2006) 501–509.
[18] L. D'Aloia Schwartzentruber, R. Le Roy, J. Cordin, Rheological behaviour of fresh cement pastes formulated from a self compacting concrete — SCC, Cement and Concrete Research 36 (2006) 1203–1213.
[19] J.E. Wallevik, Relationships between Bingham parameters and slump, Cement and Concrete Research 36 (2006) 1214–1221.
[20] A.B. Yu, R.P. Zou, N. Standish, Packing of ternary mixtures of non-spherical particles, Journal of the American Ceramic Society 75 (10) (1992) 265–272.
[21] A.B. Yu, N. Standish, A. McLean, Porosity calculation of binary mixtures of non spherical particles, Journal of the American Ceramic Society 76 (11) (1993) 2813–2816.
[22] S., Grunewald, Performance based design of self compacting steel fiber reinforced concrete", PhD Thesis, Delft University of Technology, 2004.
[23] V.K. Bui, M.R. Geiker, S.P. Shah, Rheology of fiber reinforced cementitious materials, in: A. Naaman, H.W. Rheinhardt (Eds.), Proceedings HPFRCC4, RILEM Pubs., Paris, 2003, pp. 221–231.
[24] E.N.B. Pereira, J.A.O. Barros, A.F. Ribeiro, A. Camoes, Post cracking behavior of self compacting steel fiber reinforced concrete", in: M. di Prisco, et al., (Eds.), Proceedings BEFIB04, RILEM Pubs., Paris, 2004, pp. 1371–1380.
[25] N., Ozyurt, Connecting fiber dispersion, rheology and mechanical performance for fiber reinforced cement based materials, PhD Thesis, Istanbul Technical Institute, 2005.

[26] L. Ferrara, A. Meda, Relationships between fibre distribution, workability and the mechanical properties of SFRC applied to precast roof elements, Materials and Structures 39 (2006) 411–420.
[27] J.L. Granju, V. Sabathier, M. Alcantara, G. Pons, M. Mouret, Hybrid fiber reinforcement for ordinary self compacting concrete, in: M. di Prisco, et al., (Eds.), Proceedings BEFIB04, RILEM Pubs., Paris, 2004, pp. 1311–1320.
[28] M. Alcantara, M. Mouret, G. Pons, J.L. Granju, Self compacting concrete with hybrid fiber reinforcements: workability and mechanical behaviour, in: S.P. Shah (Ed.), Proceedings SCC 2005, Hanley Wood Pub., Addison IL, 2005, pp. 423–430.
[29] ASTM C136, Standard test method for sieve analysis of fine and coarse aggregates.
[30] EN 933-1, Tests for geometrical properties of aggregates. Determination of particle size distribution. Sieving method.
[31] J.E. Funk, D.R. Dinger, Predictive Control of Crowded Particulate Suspension Applied to Ceramic Manufacturing, Kluwer Academic Press, 1994.
[32] A.H. Andreasen, J. Andersen, Ueber die beziehung zwischen kornabstufung und swischeraum in produkten aus losen körnen (mit einigen experimenten), Kolloid-Zeitschrift 50 (1930) 217–228 (in German).
[33] ASTM C29/C29M-97, Standard test method for bulk density ("unit weight") and voids in aggregate.
[34] R.P. Douglas, V.K. Bui, Y. Akkaya, S.P. Shah, Properties of self consolidating concrete containing class F fly ash: with a verification of the minimum paste volume method, ACI SP233: Workability of SCC: Role of its Constituents and Measuring Techniques, 2005, pp. 45–64.
[35] ASTM C127-04, Standard test method for density, relative density (specific gravity) and absorption of coarse aggreate.
[36] ASTM C128-04a, Standard test method for density, relative density (specific gravity) and absorption of fine aggreate.
[37] R. Gettu, D.R. Gardner, H. Saldivar, B. Barragan, Study of the distribution and orientation of fibers in SFRC specimens, Materials and Structures 38 (2005) 31–37.